University of Tennessee, Knoxville

TRACE: Tennessee Research and Creative Exchange

Chancellor’s Honors Program Projects

Supervised Undergraduate Student Research and Creative Work

Spring 5-2006

Biocompatible Microelectromechanical Sensor Array for Orthopaedic Use

Emily Pritchard
University of Tennessee-Knoxville

Follow this and additional works at: https://trace.tennessee.edu/utk_chanhonoproj

Recommended Citation

Pritchard, Emily, "Biocompatible Microelectromechanical Sensor Array for Orthopaedic Use" (2006). *Chancellor’s Honors Program Projects.*
https://trace.tennessee.edu/utk_chanhonoproj/998

This is brought to you for free and open access by the Supervised Undergraduate Student Research and Creative Work at TRACE: Tennessee Research and Creative Exchange. It has been accepted for inclusion in Chancellor’s Honors Program Projects by an authorized administrator of TRACE: Tennessee Research and Creative Exchange. For more information, please contact trace@utk.edu.

Biocompatible Microelectromechanical Sensor Array for Orthopaedic Use

Final Report

Senior Honors Project
Biomedical Engineering

Prepared by: Emily Pritchard

Submitted to: Dr. Mohamed Mahfouz

UNIVERSITY OF TENNESSEE

Table of Contents

ABSTRACT 3
INTRODUCTION 3
History of Instrumented Implant Designs 4
SENIOR DESIGN PROJECT 5
BACKGROUND 6
Sensors: Currently Marketed 6
Parylene 7
Properties of Parylene [29] 8
Parylene Deposition Technique 9
Uses for Parylene 10
EXPERIMENTAL PROCEDURE 11
Initial Wafer Investigation 12
Array Design 12
Initial Fabrication Process 13
Figure 12. Overexposure and overdevelopment of the wafer. 16
Recommended Further Experiments 16
Array Design Adjustment 17
CONCLUSION 20
REFERENCES 21

ABSTRACT

Total Knee Arthroplasty (TKA) surgeries can be significantly improved with post-operative *in vivo* feedback to the surgeon. Strain sensors incorporated into the implant itself can introduce a new generation of artificial knees, equipping surgeons with accurate feedback of intercompartmental pressures that allow the surgeon to detect malalignment, predict polyethylene wear, and make informed revision decisions.

Microelectromechanical Systems (MEMS) can be designed to be these strain sensors in the knee. Biocompatibility of the strain sensors is a key component of sensor design. However, current semiconductor manufacturing processes are not designed to accommodate most biocompatible materials. This project examines the possibility of creating a unique fabrication process for a fully biocompatible strain sensor for use in artificial knee implants.

INTRODUCTION

Knee replacement, also called Total Knee Arthoplasty has evolved since its birth in the 1960's. Artificial knees were first developed in two parallel types: anatomically designed and functionally designed [1,2]. Today the two have blended in a vast array of options. Most current designs feature separate metal components for the femur and the tibia, with a self-lubricating polyethylene insert between them. Typically artificial knee components last 8-20 years [3-5]. Knee implants today are primarily designed to mimic natural motion; designs including rotating platforms, posterior stabilized, cruciate retaining. TKA surgeries are becoming increasingly common, with 326,000 performed in 2001 in the United States which is still growing at a phenomenal rate [6].

However, the benefits of these designs are hindered by implant failure due to infection, aseptic loosening, instability, extensor mechanism deficiency, and patellar complications [7]. Implant failure requires surgical intervention, replacing the failed components with new ones (revision). Revision surgery is more invasive than primary TKA due to the damage of removing the old implant and the bone loss from cutting to fit the new implant. Revision comprises a growing 8-15% of TKA surgeries each year [8]. As the recipient population extends to include younger patients, increased activity levels also contribute to premature failure and increased revision rates [9].

Although *in vivo* data about a joint replacement is most accurate, the difficulties of cyclic loading conditions, biocompatibility, and size restraints have forced most of the study of knee loading into less accurate mathematical modeling methods.

History of Instrumented Implant Designs

Intial designs for instrumented implants focused on hip replacements and fitted them with strain gauges. In 1966, Rydell placed strain gauges on the femoral component of a hip prosthesis and passed wires through the skin for readout [10]. English, Goodman, and Kilvington used a similar setup with strain gauges, but transmitted data with an FM radio transmitter with similar findings for forces in the hip joint (Fig. 1) [11-13].

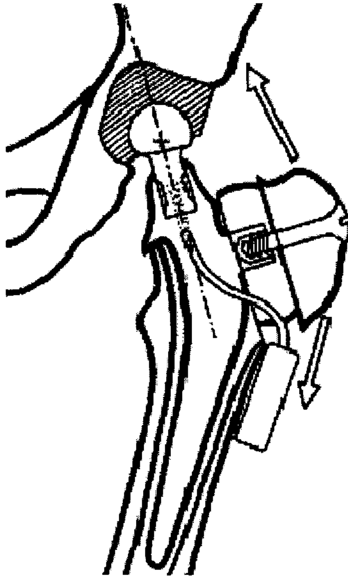

Figure 1. Telemetric Hip using FM transmitter: 1978 Design

Bergmann, Graichen, and Rohlmann built on the concepts of using strain gauges in 1988, continuing to refine the work until now. His work features an inductively-powered multi-channel output sent outside the body through an RF transmitter. The patient wears the inductive coil during measurement readings [14-19]. Davy and Kotzar also published work in 1988 for a strain-gauge hip prosthesis, with slightly lower force values during gait [20,21].

Bassey, Littlewood, and Taylor were the first to work on measuring femoral forces by extending the concept of the instrumented hip in 1997 [22-25]. A massive femoral implant was used with strain gauges in the distal intremedullary section to sense axial forces near the knee. Their implant was also inductively powered.

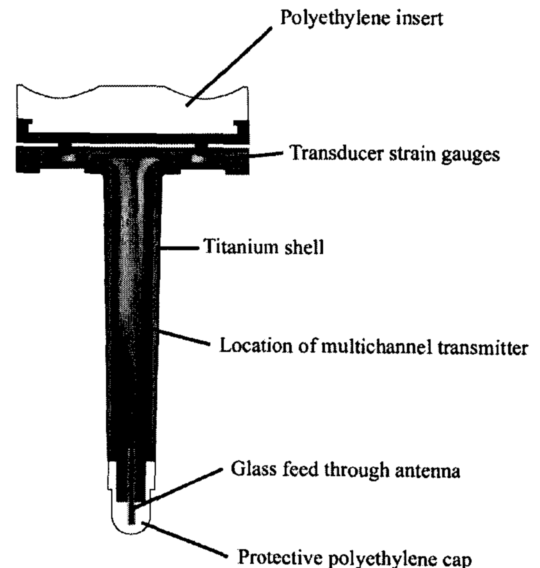

Figure 2. D'Lima and Colwell's 2005 telemetric knee design

D'Lima and Colwell of the Scripps Clinic Center for Orthopeaedic Research and Education published information in 1996 about an instrumented tibial component for measureing forces in the knee. They have continued work in collaboration with DePuy, Johnson and Johnson, Microstrain, and NK Biotechnical [26-28]. Load cells were added to the tibial tray, as seen in Figure 2, and the entire tibial component was separated into a top and bottom half to form a diaphragm for the placement of the strain gauges. The device was fabricated using off-the-shelf surface mount electronic components placed in the hollowed out areas of the implant. The instumented tibial tray allowed for measurement of axial forces only.

SENIOR DESIGN PROJECT

The complexity of the knee and its movement requires more information than simple axial loading. Femoral gliding, gliding, and external rotation occur with respect to the tibia during normal motion. However, previous instrumented implants have only accounted for the axial direction with the in-plane measurements of strain gauges and strain rosettes (see History section). To fully characterize the loading state *in vivo*, it is proposed to use MEMS sensors to measure shear frictional) forces in addition to measuring axial forces. The small size of a MEMS sensor would allow for a large array of sensors to be placed on the tibial tray or polyethylene insert to provide location specific data as well. This enables the measurement of contact areas and thus the prediction of polyethylene wear.

This senior design project investigates the feasibility of adapting semi-conductor processing techniques with biocompatible materials. Listed below are the project objectives for the senior design project to be completed from August 2005 to May 1006:

1. Design of microelectromechanical (MEMS) sensor array from single sensor unit furnished by Ph.D. student. Each sensor will be able to be individually addressed so that the pressure values at various locations can be read.

2. Design and experimentation to develop a fabrication process appropriate for the sensor with non-standard semiconductor materials- namely, biocompatible materials approved by the FDA. The sensor may not contain any material not approved for implantation, and the materials must contribute to the performance of the sensor. The fabrication process is lengthy and UT does not have the capability to do this work, so it is expected that the majority of the work will be done at Cornell University, the Oak Ridge National Laboratory, or at UT with machines purchased through proposals to support this work and other projects like it. It is expected to do as much as feasible within the academic year and to utilize as many available resources as possible.

3. Protection of the sensor array by initial experimentation with various methods of applying rigid materials to enable them to be incorporated into a knee replacement.

It is also assumed that an article will be submitted to a scholarly journal after completion of the project. As this may partially depend on the sensor cell design by a graduate student and resources available outside UT, the paper may be submitted after the undergraduate student's graduation in the summer or fall 2006.

BACKGROUND

Sensors: Currently Marketed

The sensor design patents by Tekscan (4734034, 4856993) use 2 sets of parallel electrodes on a thin, flexible supporting sheet. The electrodes are coated with thin resistive coating. The two sheet are orientated 90 degrees to each other to form a grid where the intersecting electrodes cross separated by the resistive coatings. The material between the 2 sets of electrodes should provide high resistances to the electrodes under no load conditions. Applying external pressure over the sensors will offset the resistance between the two electrodes, where it can be measured. Also, the sensor output is dynamic.

Currently, there are three major companies providing tactile sensing equipments to monitor the stress profile; Table 1 shows the comparison of some of the specifications between the sensors from each of those companies. Figure 3 shows Novel's sensing array designed for intra-operative knee use. Figure 4 shows Tekscan's knee sensor array, while Figure 5 shows the conformable and stretchable characteristics of the Pressure Profile System, which has not yet been utilized for knees.

Table 1. Specifications of Current Tactile Sensors Marketed Today

Company	No. of sensors	Sensing area	Technology	Range
Novel (Knee Pad D)	256	43mm x 43mm	Capacitance	50 – 1800kPa
Tekscan (K-Scan #4000)	1144	203mm x 203mm	Resistance	Max. range from 82.7 to 172 MPa
Pressure Profile System (Conformable TactArray T-2000)	unknown	300mm x 300mm	Capacitance	1400 kPa

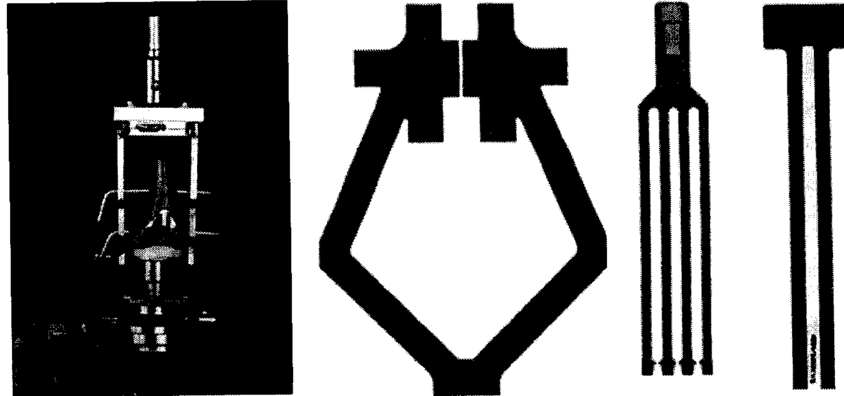

Figure 4. Tekscan knee sensor arrays

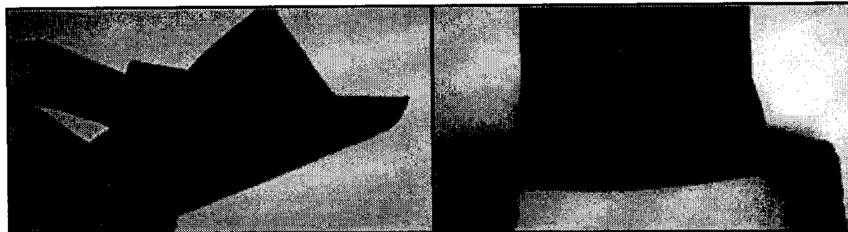

Figure 5. Pressure Profile, Inc. conformable (left) and stretchable (right) sensor arrays

Parylene

The primary biocompatible material considered for MEMS fabrication is poly-para-xylylene, known primarily by its trade name, parylene. Para-xylene is available in types C, D, and N (Fig. 6). Parylene C (para-chloroxylylene) is approved by the U.S. Food and Drug Administration for multiple implantation purposes. It has been used in the semiconductor industry for its molecularly smooth surfaces that are pin-hole free. This also allows parylene to protect a metal from a corrosive environment- it is very inert. Its moisture barrier properties and gas transmission are a key for its sealant applications as well (Table 2). Its mechanical properties are extremely predictable due to coatings free of mechanical and thermal stresses. Parylene has been used as a dielectric and as an insulator because of its superior electrical properties (Table 4). Because of its optical properties and smooth coating, it has also been used on high performance mirrors (Table 6).

Parylene N

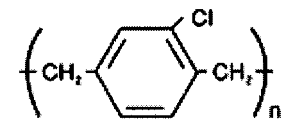

Parylene C

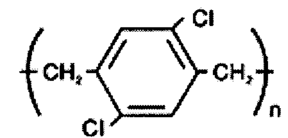

Parylene D

Figure 6. Types of Parylene

Properties of Parylene [29]

Table 2. Physical Properties	Metric	English	Other
Density	1.289 g/cc	0.0466 lb/in³	
Water Absorption	0.06 %	0.06 %	0.029 inches; 24 hrs.
Moisture Vapor Transmission	0.0551 cc-mm/m²-24hr-atm	0.14 cc-mil/100 in²-24hr-atm	37°C; 90% RH
Oxygen Transmission	2.8 cc-mm/m²-24hr-atm	7.1 cc-mil/100 in²-24hr-atm	23°C
Nitrogen Transmission	0.374 cc-mm/m²-24hr-atm	0.95 cc-mil/100 in²-24hr-atm	23°C
Carbon Dioxide Transmission	3.03 cc-mm/m²-24hr-atm	7.7 cc-mil/100 in²-24hr-atm	23°C
Hydrogen Sulfide Transmission	5.12 cc-mm/m²-24hr-atm	13 cc-mil/100 in²-24hr-atm	23°C
Sulfur Dioxide Transmission	4.33 cc-mm/m²-24hr-atm	11 cc-mil/100 in²-24hr-atm	23°C
Chlorine Transmission	0.138 cc-mm/m²-24hr-atm	0.35 cc-mil/100 in²-24hr-atm	23°C

Table 3. Mechanical Properties

Tensile Strength, Ultimate	68.9 MPa	10000 psi	
Tensile Strength, Yield	55.2 MPa	8000 psi	
Elongation at Break	200 %	200 %	
Elongation at Yield	2.9 %	2.9 %	
Tensile Modulus	3.2 GPa	464 ksi	
Coefficient of Friction	0.29	0.29	Dynamic
Coefficient of Friction, Static	0.29	0.29	

Table 4. Electrical Properties

Volume Resistivity	6e+016 ohm-cm	6e+016 ohm-cm	50% RH
Surface Resistance	1e+015 ohm	1e+015 ohm	50% RH
Dielectric Constant	2.95	2.95	1 MHz
Dielectric Constant	3.1	3.1	1 kHz
Dielectric Constant, Low Frequency	3.15	3.15	60 Hz
Dielectric Strength	268 kV/mm	6800 V/mil	Short Time; 1 mil
Dissipation Factor	0.013	0.013	1 MHz

Table 5. Thermal Properties

CTE, linear 20°C	35 μm/m-°C	19.4 μin/in-°F	
Thermal Conductivity	0.082 W/m-K	0.569 BTU-in/hr-ft^2-°F	
Melting Point	290 °C	554 °F	
Maximum Service Temperature, Air	125 °C	257 °F	Continuous

Table 6. Optical Properties

Refractive Index	1.639	1.639	
Transmission, Visible	90 %	90 %	Optically clear, but reports do not quantify.

Parylene Deposition Technique

Parylene is primarily deposited at room temperature using a chemical vapor deposition (CVD) process (Fig. 7). Dimer pellets of parylene are placed in a boat and are vaporized at 150° C in a vacuum. The vapor is then pyrolized to separate it into the monomer form. The deposition chamber at room temperature also contains the items to be coated, and the parylene vapor polymerizes on all surfaces of the deposition chamber. Excess parylene is removed from the chamber by a cold finger, where it condenses and can be removed after the coating process. The entire process takes approximately five hours.

Sensors to detect actual deposition thickness have been developed [30], but for the purposes of this project it is possible to gauge the deposition thickness by accurately measuring the initial dimer amount. A test wafer with the desired dimer amount can then be peeled or cut at various intervals and measured to provide a reliable thickness estimate.

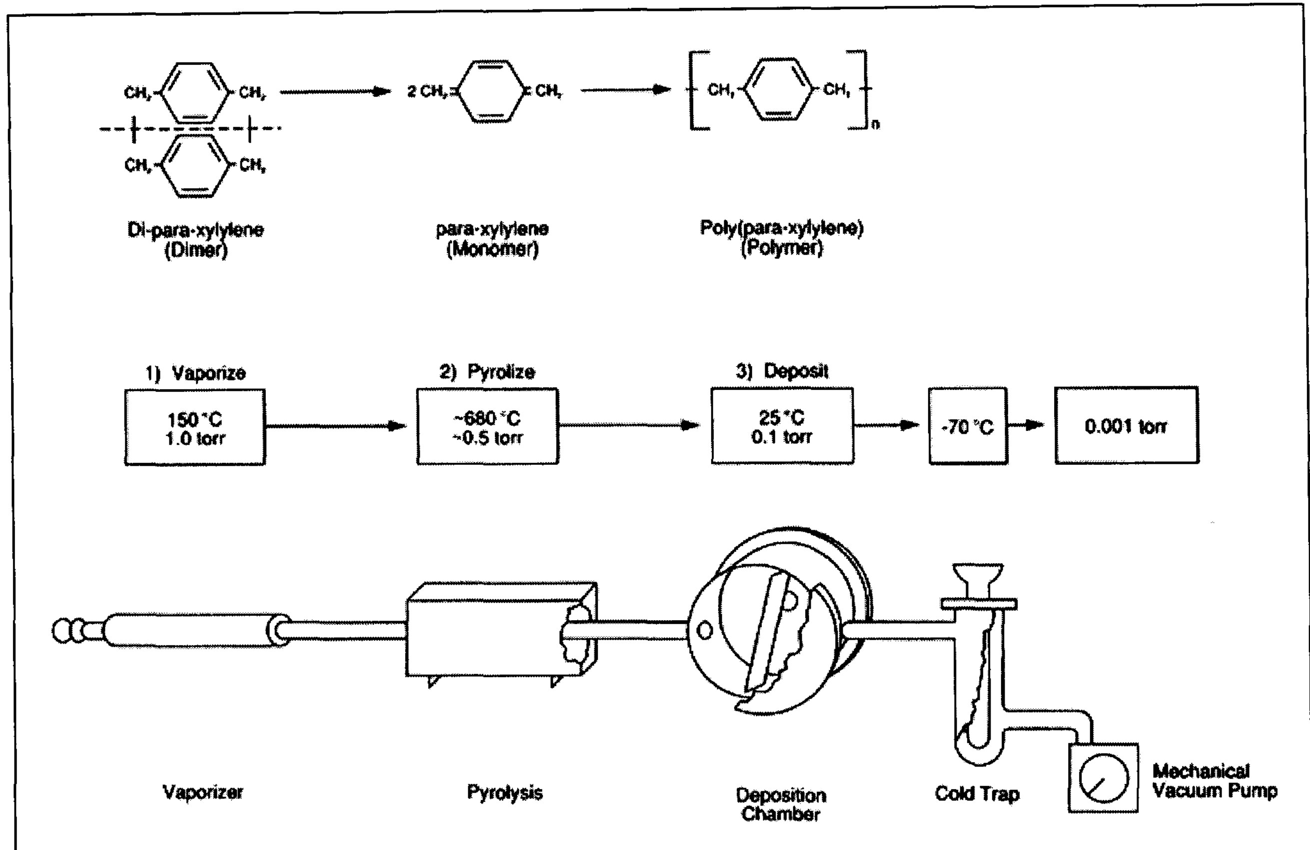

Figure 7. Parylene Deposition Schematic [31]

Uses for Parylene

- Microvalves [32]
- Microelectrode Insulator [33]
- Pacemakers [34]
- Neurocages [35]
- Protein chips [36]
- Dielectric films [37]
- Cochlear, retinal, penile, and neural implants [38-42]
- Microfluidic applications [42-43]
- Hermetic sealing [45]
- Biomedical blood pressure sensors [45,46]
- Intravascular sensors [47]
- Corrosion protection [48]
- Membranes [49]
- Miniature gas chromatograph [50]
- Acoustic transducers [51]
- Potential difference probes [52]
- Optical scanners on the micro- scale [53]
- Peristaltic pumps [54]

EXPERIMENTAL PROCEDURE

A fabrication procedure was established for fabrication of all layers of the sensor. This included three masks and 3-4 separate photolithography steps. Three parylene coatings were included: base layer, dielectric layer (with interconnects) and a top, sealing layer. Figure 8 shows the total proposed fabrication process.

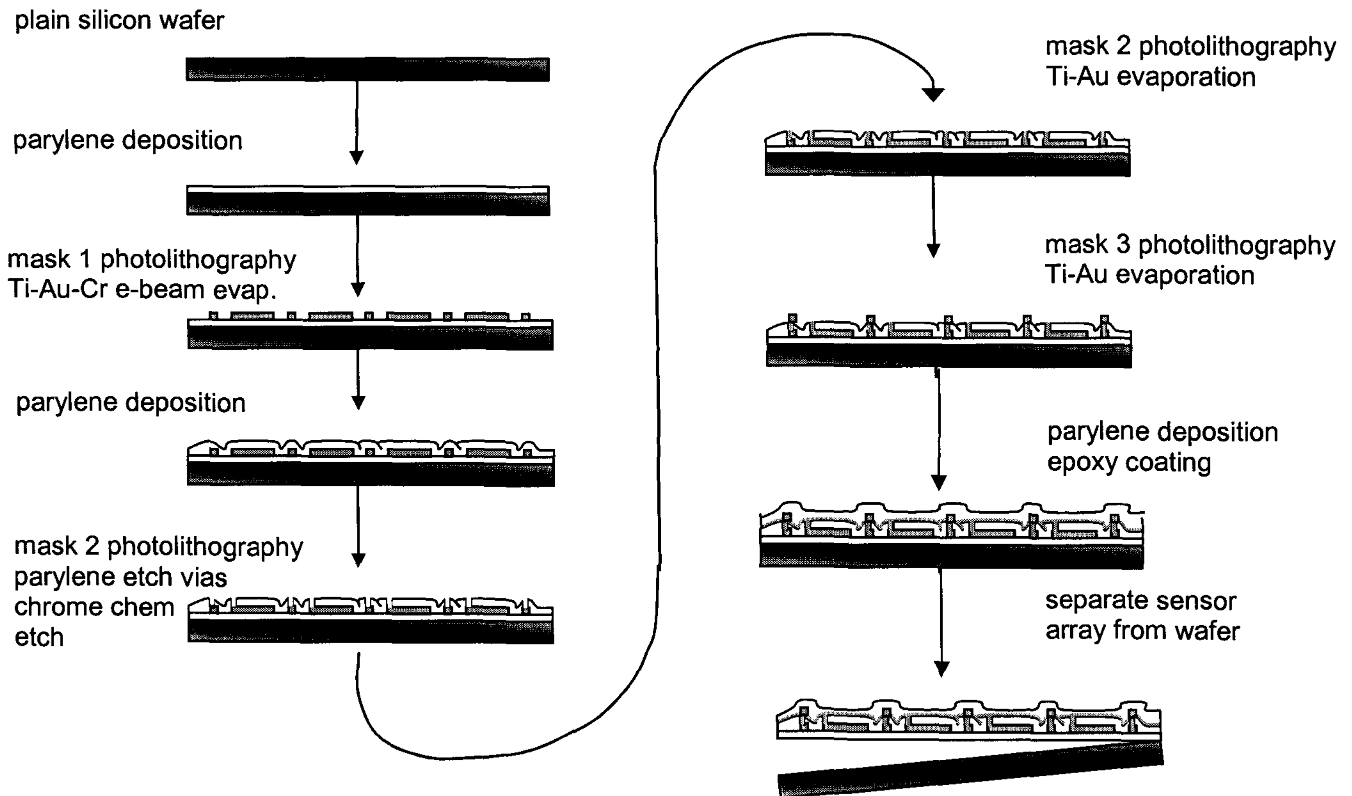

A test set of wafers was fabricated to gain insight to the microfabrication process and to establish what questions and problems are pertinent to the problem at hand. Further experiments are based on preliminary experimental outcomes and are intended to be smaller scale to inform before another large-scale, expensive fabrication run. After preliminary experiments, a test sample will be fabricated (Fig. 8).

In order to accomplish these goals, training at was completed at Cornell Nanoscale Facility (CNF) at Cornell University, Ithaca, NY. All array fabrication for the initial wafer investigation was done at CNF.

Initial Wafer Investigation

Array Design

The first layer of the initial sensor design was obtained from the graduate student and was designed into an array using L-Edit by Tanner EDA. Each cell contained two interdigitated sensors to measure shear forces and one parallel plate capacitor for sensing in the axial direction (Figure 8). Each of these sensors needed to be individually accessed, and it was crucial to know the position of the sensor being read. An addressing system was used to identify each individual sensor in the array. Bond pads were provided at the edges of the array connecting to each trace, with size large enough for soldering (.5 mm × .5 mm). Wire-bond pads were not used because of the concern that during the wirebond process the parylene base layer may be penetrated, yielding a broken trace/bond interface. The ends of the traces for each individual cell were enlarged so that when patterning any small error in mask alignment would still allow the traces to connect. This is also crucial for the alignment of different layers, as the alignment may be off a micron and interconnects need to ensure signal transduction.

A second mask design was created to reduce the number of traces by a factor of 4. Each group of 4 cells were joined so that instead of 12 leads coming out, only 3 were needed for that group (Figures 10 and 11). This has the effect of canceling some noise in the signal, as well as amplifying the signal, since the readout capacitance change is so small it is difficult to detect even with specialized readout circuitry. The sensor dimensions were not reduced for this mask.

A soda-lime chrome mask was created with the array design of layer 1 on a Hiedelberg Direct-Write Laser 66. The mask was then developed and cleaned prior to use with wafers.

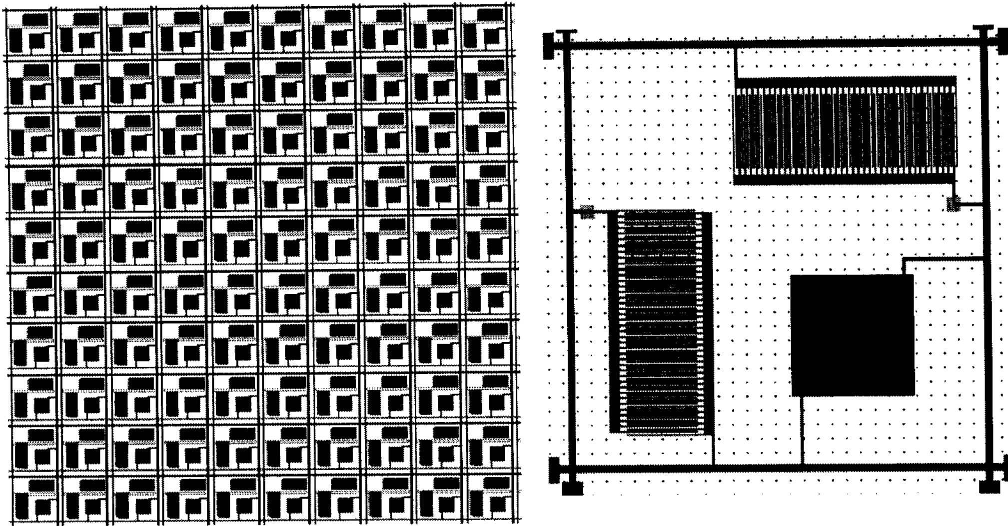

Figure 8. Original Sensor Array (left) and cell (right)

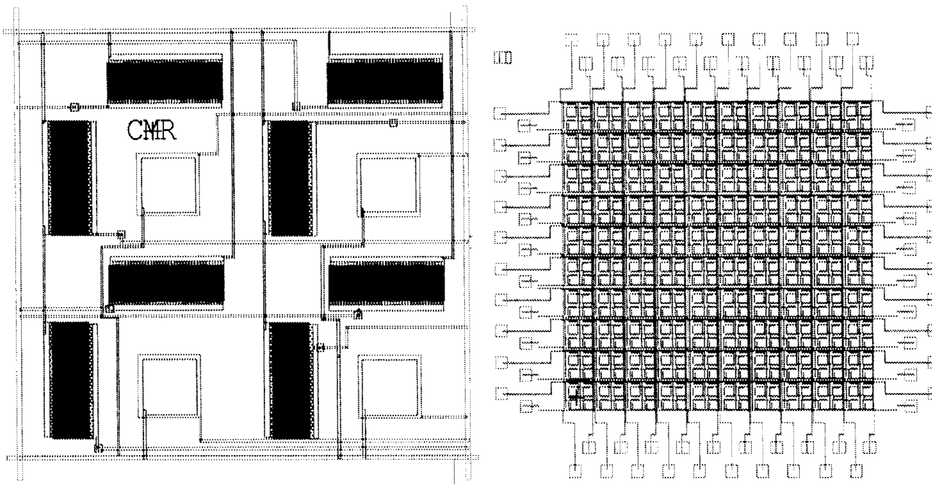

Figure 9. Sensor cell (left) and array (right) for secondary design using 4 cells connected together.

Initial Fabrication Process

All wafers used were individually labeled with a diamond scribe. Twelve wafers were cleaned in a hot nanostrip bath. Four wafers underwent cleaning in a Pirhana recipe of hydrogen peroxide and sulfuric acid. A base layer of parylene was deposited onto 4 silicon wafers using 2 batches in a PDS 2010 Labcoter. Half a gram of dimer was used for both batches to ensure equal parylene depth. As this was a base layer, the actual thickness of the parylene layer was not crucial and was not measured. However, training was completed on a Tencor P10 Profilometer for future measurement of parylene thickness.

Photoresist was then manually spun onto the wafers. Shipley 1818 positive photoresist was used after a liquid HMDS priming step. The 4 wafers originally cleaned with Pirhana were not satisfactorily spun due to inexperience of the user and were

subsequently cleaned with methanol, isopropyl alcohol (IPA) and acetone. However, because of the repeated failure to spin the photoresist and thus the repeated cleanings, the wafers were subjected to a hot nanostrip to remove the photoresist completely and start over. All 12 wafers were cleaned in 1 batch in the hot nanostrip bath for the same length of time. The wafers were then successfully

A second batch of 4 wafers in the parylene coater was completed using .5 grams of dimer and the wafers successfully coated with photoresist through the manual spinning process described above. A soft bake for 30 seconds at 90° Celsius was used to remove excess solvent from the photoresist prior to exposure.

The mask was then loaded into an EVG 620 contact aligner and initial exposure tests performed. A total of 5 exposure tests were completed. No image reversal was performed on the exposure wafers to save time, with the assumption that the ideal exposure time would not change much with image reversal. The first pair of wafer exposure tests were the same, varying the exposure time from .5 to 3 seconds in .5 second intervals. However, exposure test 1 was developed in MF 300 developer (single puddle) and exposure test 2 was developed in MF 321 developer (double puddle). Both were developed for 60 seconds in a Hamatech automated developer. The time interval chosen for these tests was large in order to narrow down the range of possible exposure times. Under microscope inspection, it was evident that the ideal exposure time was between 1 and 3 seconds of exposure (2.5 seconds appeared to be best). Since the two exposure tests were identical except for the developer used, it could also be shown that MF 321 produced better results. Another wafer was tested from .6 to 2.4 seconds of exposure (.3 second intervals) and developed in MF 321 for 60 seconds. The smaller interval was designed to narrow down the best exposure time, since on previous test wafers the ideal time ranged between 1.5 and 2.5. Because 2 seconds looked best on the third test wafer, the subsequent exposure tests were put back to a .5 second time interval. The fourth and fifth wafers were tested from 1 to 3 seconds at .5 second intervals, with one developed in MF 300 and one developed in MF 321. This was done because of inexperience with the process, and the apparent success of MF 321 over MF 300 (MF 300 was recommended, while MF 321 was not). Based on the lengthy exposure tests, 2 seconds exposure was decided for use. Figure 10 shows a exposure test wafer. The bands correspond to different exposure times.

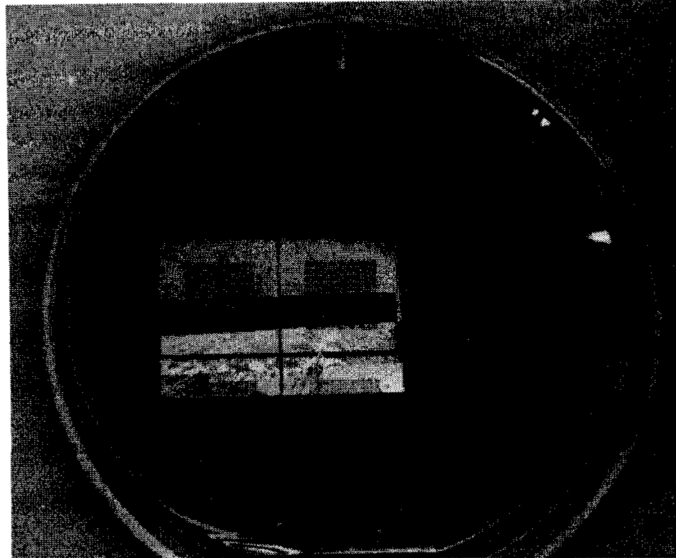

Figure 10. Exposure test wafer, showing bands corresponding to different exposure times.

Two wafers coated in parylene were exposed for 2 seconds using the EVG 620 and the small array mask. The wafers were then put in a YES Ammonia oven (1.5 hours) for image reversal. They were then flood exposed for 10 seconds, developed using the MF 321 protocol, and examined. Both samples looked very good under microscope inspection, but it was judged that there was some excess photoresist left in the patterned areas (very hard to see, and for the untrained eye, hard to tell.). Figure 11 shows the wafer at this point. Both samples were then exposed for an additional 5 seconds and developed again in MF 321 for 60 seconds to remove any excess photoresist. However, this caused the fingers of the interdigitated sensors to lift off the wafer, giving a wavy appearance (Figure 12).

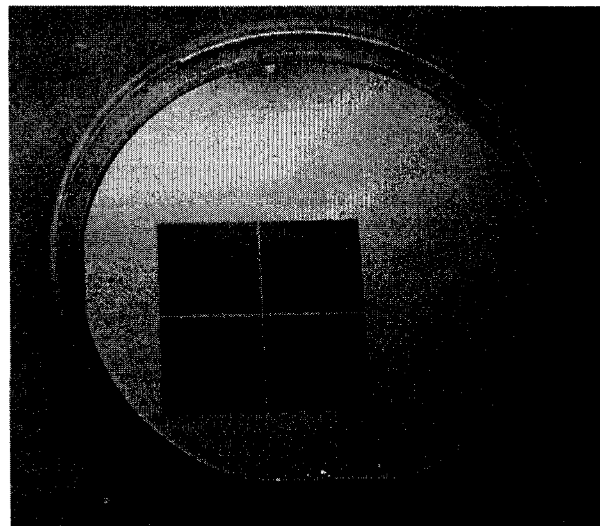

Figure 11. Wafer after image reversal, flood exposure, and development. Each square is one array of approximately 400 sensors.

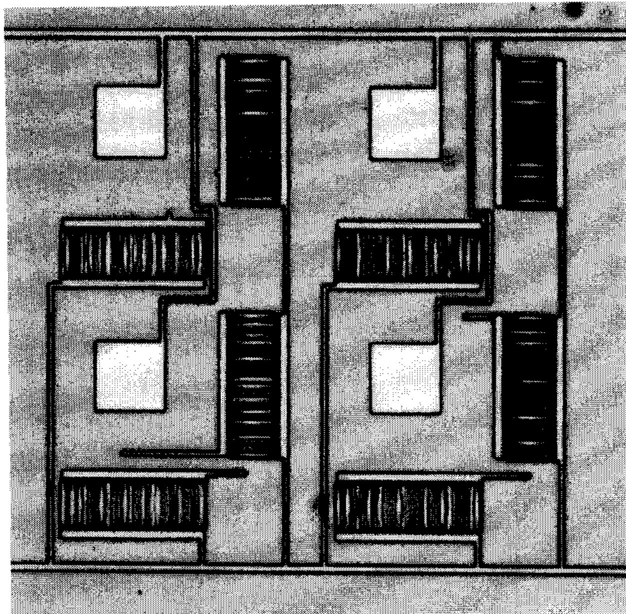

Figure 12. Overexposure and overdevelopment of the wafer.

Recommended Further Experiments

Based on the results from the initial wafer fabrication (layer 1 only), further recommended experiments were constructed.

- Verify parylene etch rates
  - Compare to published values
  - 4 wafers
  - 10 readings per wafer with contact profilometer or AFM
    - average etch distance
- Investigate use of lift-off resists
  - AZ5214 lift-off resist
- Optimize exposure and development time for given feature geometry and size (once specified by cell design)

Array Design Adjustment

The cell design had been modified by the graduate student to include 6 sensors per cell, doubling the complexity for incorporation into an array. Two possible scenarios were formulated using the same addressing concept as in the original array (Figures 13 and 14).

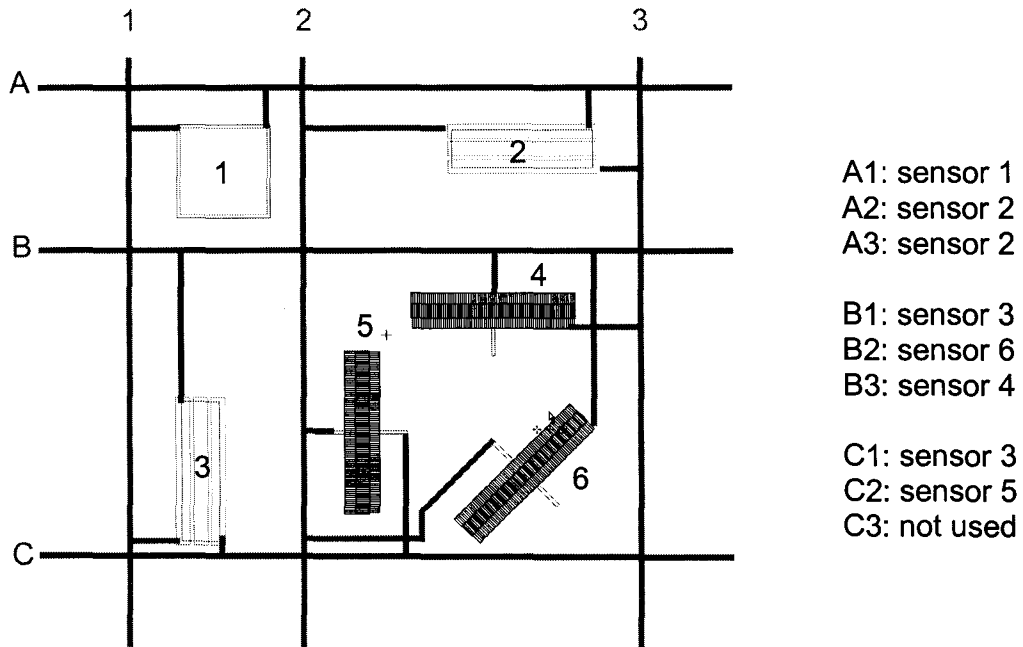

Figure 13. Addressing scheme possibility for new cell design. Single cell shown. Different colors designate different layers.

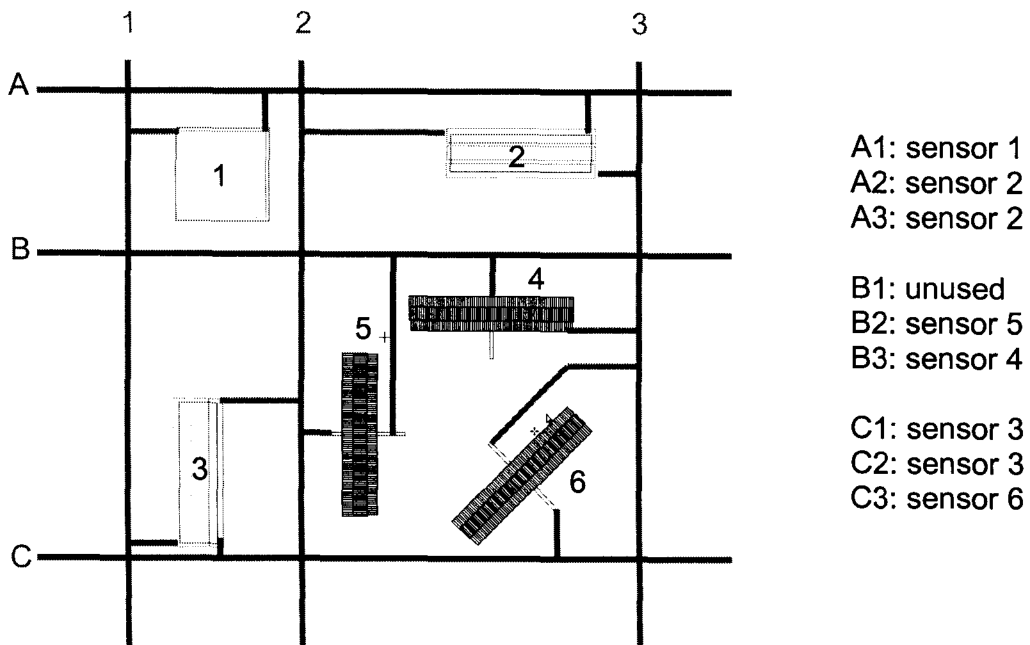

Figure 14. Addressing scheme possibility for new cell design. Single cell shown. Different colors designate different layers.

The width and separation of the traces is an important factor in reducing noise from the output signal. If the wires are located too close together, patasitic capacitance is produced between them when one wire is excited. The width of the wires determines the current density and the rersistance of the leads (heat produced). Three cases should be examined as shown in Figure 15. The first two cases were examined using 2D simulation for the arbitrary sensor width and separation chosen for the first iteration of fabrication (Figure 16). The results showed significant electric field only at the ends of the wires, signifying a parasitic capacitance between the wires only at these points. More investigation is needed, particularly using the complex sensor geometry to further understand the effect. The third case of crosstalk, wires crossing on different layers, requires a 3D simulation and is more difficult. Once the simplified cases are completed in simulation, simulation of the actual sensor array should be performed.

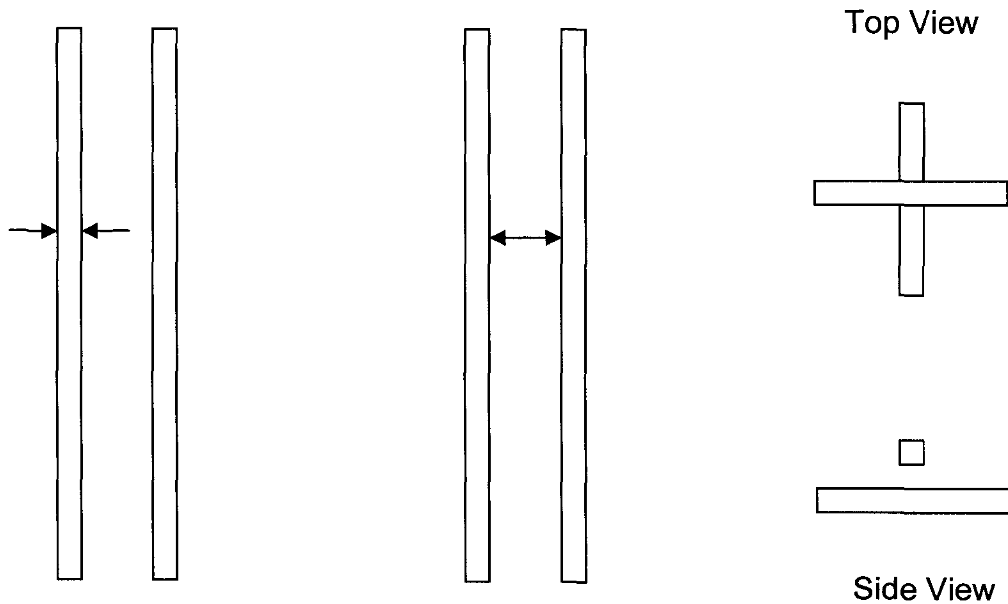

Figure 15. Scenarios of crosstalk between trace configurations. Wire width (left), wire separation (middle) and wire crossing on different layers, parylene as the dielectric (right).

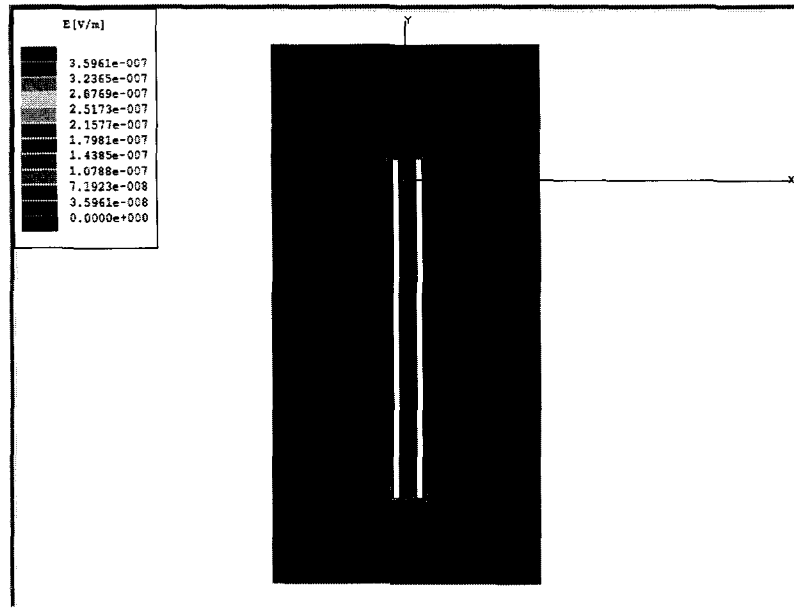

Figure 16. Representative Maxwell 2D simulation of wire width and separation.

CONCLUSION

Using semiconductor microfabrication technology, it is possible to modify current processes to accommodate biocompatible materials. The use of all biocompatible materials (approved by the Food and Drug Administration) for the fabrication of a pressure sensor has been achieved. Further simulation and experimental testing are needed to optimize the fabrication of a biocompatible sensor array. Significant strides have been made in optimizing the first iteration of design and identifying areas for future concentration.

An implantable sensor array would be clinically relevant for surgeons across the globe to detect malalignment, predict polyethylene wear, and make informed revision decisions for both intra-operative and post-operative feedback for joint replacement. The potential for high accuracy and increased spatial resolution make microelectromechanical sensors a promising method of achieving these clinical goals.

REFERENCES

[1] R.P. Robinson. "The early innovators of today's resurfacing condylar knees." 2005. J. Arthroplasty. 20(1 Suppl 1): 2-26.

[2 C.S. Ranawat. "History of Knee Replacement." 2002. J South Orthop Assoc. Winter 11(4): 218-26

[3 Buechel Sr, FF. Long-Term Followup After Mobile-Bearing Total Knee Replacement. Clin Orthop 404: 40-50, 2002.

[4] Pavone V, Boettner F, Fickert S, Sculco TP. Total Condylar Knee Arthroplasty: A Long-Term Followup. Clin Orthop 368: 18-25, 2001.

[5] Rodriguez JA, Bhende H, Ranawat CS. Total Condylar Knee Replacement A 20-Year Followup Study. Clin Orthop 388: 10-17, 2001.

[6] National Hospital Discharge Summary 2001. National Center for Health Statistics. http://www.cdc.gov/nchs/data/series/sr_13/sr13_156.pdf

[7] Sharkey PF: Why are total knee arthroplasties failing today? Clin Orthop 404: 7-13, 2002.

[8] Nationwide Inpatient Survey 1997. National Center for Health Statistics. http://www.cdc.gov/nis

[9] Diduch DR, Insal JN, Scott WN, Scuderi GR, Font-Rodriguez D. Total Knee Replacement in Young, Active Patients. Long-Term Follow-up and Functional Outcome. J Bone Joint Surg Am. 79:575-582, 1997.

[10] Rydell NW. Forces acting on the femoral head-prosthesis. A study on strain gauge supplied prostheses in living persons. Acta Orthop Scand. 1966;37:Suppl 88:1-132

[11] R.M.F. Goodman, T.A. English, M. Kilvington. "An implantable FM Telemetry system for measuring forces on prosthetic hip joints." 1979. *A handbook on biotelemetry and radio tracking*, Pergamon Press, Oxford: 297-306

[12] T.A. English, M. Kilvington. "A methods for measurement of hip loads using a strain-gauged implant with telemetric output." 1980. *Evaluation of Bio-Materials.* John Wiley and Sons, Chichester: Ch. 7

[13] M. Kilvington, R.M.F. Goodman. "In vivo hip joint forces recorded on a strain gauged 'English' prosthesis using an implanted transmitter." 1981. *MEP Ltd.* Vol.10 No. 4: 175-187

[14] Bergmann G. Graichen F. Rohlmann A. Instrumentation of a hip joint prosthesis. In: Bergmann G, Graichen F, Rohlmann A (Eds.). Implantable Telemetry in Orthopaedics. Forshungsvermittlung der Freien universitat, Berlin, 35-63.

[15] Graichen F, Bergmann G, Rohlmann A. Inductively powered telemetry system for in vivo measurement with orthopedic implants. In: Cristalli, Amlaner, Neuman (Eds.), Thirteenth International Symposium on Biotelemetry, Williamsburg, Vol. XIII: 75-80. Biotelemetry

[16] Graichen F, Bergmann G. Four-channel telemetry system for in vivo measurement of hip joint forces. Journal of Biomedical Engineering 13, 370-374, 1991.

[17] Bergmann G, Graichen F, Rohlmann A, Verdonschot N, van Lenthe GH. Frictional heating of total hip implants. Part 1. measurements in patients. Journal of Biomechanics 34;421-428, 2001.

[18] Bergmann G. Hip Joint Loading During Walking and Running Measured in Two Patients, Journal of Biomechanics 26 (8): 969-990, 1993.

[19] Bergmann G, Graichen F, Rohlmann, A, Verdonschot N, van Lenthe GH. Frictional heating of total hip implants. Part 1. measurements in patients. Journal of Biomechanics 34: 421-428, 2001.
[20] Kotzar GM, Davy DT, Goldberg VM, Heiple KG, Gerilla J, Heiple KG Jr, Brown RH, Burstein AH. Telemeterized In Vivo Hip Joint Force Data: A Report on Two Patients After Total Hip Surgery. Journal of Orthopaedic Research 9 (5): 621-633, 1989.
[21] Davy DT, Kotzar GM, Brown RH, Heiple KG, Goldberg VM, Heiple KG Jr., Berilla J, Burstein AH. Telemetric Force Measurements Across the Hip after Total Arthroplasty. Journal of Bone and Joint Surgery 70-A (1): 45-50, 1988.
[22] Bassey, E.J., Littlewood, J.J., Taylor, S.J.G., 1997. Relations between compressive axial forces in an instrumented massive femoral implant, ground reaction forces, and integrated electromyographs from vastus lateralis during various osteogenic exercises. J. Biomechanics 30, 213–223.
[23] Taylor, S.J.G., Walker, P.S., 2001. Forces and moments telemetered from two distal femoral replacements during various activities. J. Biomechanics 839–848.
[24] Taylor, S.J.G., Walker, P.S., Perry, J.S., Cannon, S.R.,Woledge, R., 1998. The forces in the distal femur and the knee during walking and other activities measured by telemetry. J. Arthroplasty 13, 428–437.
[25] Taylor, S.J.G., Walker, P.S., 2001. Forces and moments telemetered from two distal femoral replacements during various activities. J. Biomechanics 839–848.
[26] Kaufman KR, Kovacevic N, Irby SE, Colwell CW. Instrumented Implant for Measuring Tibiofemoral Forces. J. Biomechanics Vol. 29. No 5: 667-671, 1996.
[27] Morris BA, D'Lima DD, Llamin J, Kovacevic N, Arms SW, Townsend CP, Colwell CW. e-Knee: Evolution of the Electronic Knee Prosthesis Telemetry Technology Development. J Bone Joint Surg Am. Vol. 83A. Supplement 2, Part 1. 62-66, 2001.
[28] D'Lima DD, Townsend CP, Arms SW, Morris BA, Colwell CW. An implantable telemetry device to measure intra-articular tibial forces. J Biomechanics (38) 299-304, 2005.
[29] MatWeb Material Property Data. "PCS Parylene C." 2005. http://www.matweb.com/search/SpecificMaterial.asp?bassnum=PPARYLC
[30] W. Sutomo, X. Wang, D. Bullen, S.K. Braden, C. Liu. "An In-Situ End-Point Detector For Parylene CVD Deposition." 2003. IEEE Micro Electro Mechanical Systems, Kyoto: 598-601
[31] Cookson Specialty Coating Materials. "Parylene Knowledge: Specifications and Properties." 2004. http://www.scscookson.com/parylene_knowledge/specifications.cfm
[32] R. Duggirala and A. Lal. "A Hybrid PZT-Silicon Microvalve." 2005. J. of Microelectromechanical Systems. Vol. 14 No.3: 488-497
[33] G.E. Loeb, M.J. Bak, M. Salcman, E.M. Schmidt. "Parylene as a chronically stable, Reproducible Microelectrode Insulator." 1977. IEEE Trans. Biomed. Engr., 24(2):121
[34] M. Nagl, T. Lechleitner. "Barrier coatings for medical electronic implants." 2005. Vakuum in Forschung und Praxis Vol. 17, Issue S1: 47 - 50
[35] A. Tooker, E. Meng, J. Erickson, Y.C. Tai, J. Pine. "Development of Biocompatible Parylene Neurocages." 2004. IEEE EMBC 2004, San Francisco, California, USA[36] K.S. Hwang, J.H. Lee, J.H. Park, T.S. Kim. "Effect of various surface

treatment for enhancing adhesion of Au on parylene coated protein chip." 2003. *Plasma Science*: 291

[37] L.V. Gregor. "Polymer dielectric films" 1968. IBM J. of Research and Development

[38] J.R. Parker, H.P. Harrison, G.M. Clark, J. Patrick, O. Rienhold. "Development of silicon microelectrodes for cochlear implant technology." 1996. Optoelectronic and Microelectronic Materials And Devices, Canberra, Australia: 12-15

[39] H. Chun, S.J. Kim. "Development of Silicon-micromachined Retinal Tacks for Artificial Retina Implantation." 2003. 1st Intl. IEEE EMBS Conf. on Neural Engr., Capri Island, Italy: 185-188

[40] M. Okandan, K. Wessendorf, T. Christenson, T. Lemp. "MEMS Conformal Electrode Array for Retinal Implant." 2003. 12th Intl. Conf. on Solid State Sensors, Actuators, and Microsystems: 1643-1646

[41] J.J. Mulcahy, E. Austoni, J.H. Barada, H.K. Choi, et al. "The Penile Implant for Erectile Dysfunction." 2004. *J. of Sexual Medicine* Vol. 1 Issue 1: 98

[42] S.T. Retterer, K.L. Smith, C.S. Bjornsson, K.B. Neev. "Model Neural Prostheses With Integrated Microfluidics: A Potential Intervention Strategy for Controlling Reactive Cell and Tissue Responses." 2004. IEEE Transactions on Biomed. Engr. Vol. 51, No. 11: 2063-2073

[43]H.S. Noh, Y. Huang, P.J. Hesketh. "Parylene micromolding, a rapid and low-cost fabrication method for parylene microchannel." 2004. *Sensors and Actuators* B 102: 78-85

[44] B.P. Gogoi, C.H. Mastrangelo. "A low-voltage force-balanced pressure sensor with hermetically sealed servomechanism." 1999. Micro Electro Mechanical Systems

[45] B.P. Gogoi, C.H. Mastrangelo. "A low-voltage force-balanced pressure sensor with hermetically sealed servomechanism." 1999. *Micro Electro Mechanical Systems*

[46]T Eggers, C Marschner, U Marschner, B Clasbrummel. "Advanced Hybrid Integrated Low-Power Telemetric Pressure Monitoring System for Biomedical Applications." 2000. MEMS2000, Miyazaki, Japan: 329-334

[47]J.M. Schmitt, M. Baer, J.D. Meindl, M.F. Anderson, F.G. Mihm. "Inhibition of thrombus formation on intravascular sensors by electrical polarization."

[48] H. Yasuda, B.H. Chun, D.L. Cho, T.J. Lin. "Interface-Engineered Parylene C Coating for Corrosion Protection of Cold-Rolled Steel." 1996. *Corrosion* Vol. 52 No. 3: 169

[49] X. Yang, J.M. Yang, X.Q. Wang, E. Meng, Y.C. Tai, C.M. Ho. "Micromachined membrane particle filters." 1998. IEEE Eleventh Annual Intl. Workshop on MEMS '98, Heidelberg, Germany: 137-142

[50] H.S. Noh, P.J. Hesketh, G.C. Frye-Mason. "Heating element embedded Parylene microcolumn for miniature gas chromatograph." 2002. 15th Int. Conf. Micro Electro Mechanical Systems: 73-76

[51] C.H. Han, E.S. Kim. "Parylene-Diaphragm Piezoelectric Acoustic Transducers." 2000. IEEE MEMS, Miyazaki, Japan: 148-152

[52] M. Moorman, P. Hesketh, J. Zheng, S. Danyluk. "A novel, micro-contact potential difference probe." 2003. Sensors and Actuators B Vol. 94, No. 1: 13-26

[53] J.M. Zara, S.W. Smith. "Optical scanner using a MEMS actuator." 2002. Sensors and Actuators A 102: 176-184

[54] J. Xie, J. Shih, Q. Lin, B. Yang, Y.C. Tai. "Surface micromachined electrostatically actuated micro peristaltic pump." 2004. Lab on a Chip 4(5): 495-501